Research Square

Preprints are preliminary reports that have not undergone peer review.
They should not be considered conclusive, used to inform clinical practice,
or referenced by the media as validated information.

Coupling Nano-Enhanced Activated Carbon Adsorption with Multi-Model Machine-Learning Sedimentation Forecasting: A Translational Engineering Framework for the Descolmatation of Rivers, Lakes and Lagoons, from United States Practice to the Peruvian Andes

PAUL RICARDO PRUDENCIO GALVEZ

pprudencio@autonoma.edu.pe

UNIVERSIDAD AUTONOMA DEL PERU https://orcid.org/0009-0000-1986-590X

Systematic Review

Keywords: emerging contaminants, nano-enhanced activated carbon, multi-model machine learning, sedimentation prediction, descolmatation of rivers, lakes and lagoons, Andean water bodies, translational engineering

Posted Date: July 15th, 2026

DOI: https://doi.org/10.21203/rs.3.rs-10338191/v1

License: This work is licensed under a Creative Commons Attribution 4.0 International License.
Read Full License

Additional Declarations: The authors declare no competing interests.

Abstract

Emerging contaminants (ECs) and heavy-metal loads continue to accumulate in rivers, lakes and lagoons worldwide, while conventional treatment trains rarely address the coupled problems of micropollutant adsorption and progressive channel sedimentation. This Method Article synthesizes documented evidence on nano-enhanced activated carbon (AC) adsorption and multi-model machine-learning (ML) sedimentation forecasting, and proposes an integrated engineering framework that links the two processes through a shared set of governing formulas: the Langmuir adsorption isotherm, a modified Stokes' law for nano-agglomerate settling, and a weighted multi-model ML ensemble for settling-velocity prediction. Quantitative benchmarks compiled from peer-reviewed, DOI-verified sources indicate adsorption efficiencies of 60–99% for composite activated-carbon materials against pharmaceuticals, endocrine disruptors and per- and polyfluoroalkyl substances, correlation scores above R = 0.936 for tree-based multi-model ensembles in sediment-transport prediction, and heavy-metal pollution indices in Peru's Rimac basin exceeding critical contamination thresholds by more than an order of magnitude. Building on this evidence base, constructive procedures, tools and materials used in United States full-scale deployments are compared against a proposed low-cost, modular configuration adapted to the topography, hydrology and resource constraints of Andean rivers, lakes and lagoons in Peru. The framework is presented as a design and synthesis proposal rather than as a validated field trial; experimental verification with Peruvian field data is identified as a necessary next step. No human or animal subjects were involved, and no primary biological or clinical data were collected.

1. Introduction

Pharmaceuticals, personal-care products, endocrine disruptors and per- and polyfluoroalkyl substances (PFAS) are now routinely detected in surface waters at nanogram-to-microgram-per-litre concentrations, and conventional treatment trains are frequently ineffective at removing them (Chen et al., 2026). Activated carbon (AC) remains the most mature adsorbent for such micropollutants, and its performance can be substantially enhanced through composites with nanomaterials — metal or metal-oxide nanoparticles, graphene oxide, carbon nanotubes and zero-valent iron — which introduce catalytic, magnetic or highly selective adsorption sites (Chen et al., 2026; Bagheri et al., 2017; Babaee et al., 2018).

In parallel, river, lake and lagoon systems in mining-influenced watersheds accumulate sediment and heavy metals that must be periodically removed through descolmatation works. Predicting the settling behaviour of this sediment — particularly once it is mixed with spent nano-enhanced AC flocs — has moved from single empirical equations toward multi-model machine-learning (ML) ensembles that combine several algorithms (random forest, gradient boosting, extreme learning machines, long short-term memory networks) to reduce predictive uncertainty (Le et al., 2024; Sharafati et al., 2020; Achite et al., 2025).

Gap and contribution. The adsorption-materials literature and the sediment-transport ML literature have developed largely in parallel, with few frameworks that treat nanoscale adsorption performance and

macroscale settling prediction as a single, jointly engineered system. This is a significant limitation for descolmatation projects, where spent adsorbent flocs directly alter the settling dynamics that downstream sedimentation infrastructure must handle. The contribution of this article is threefold: (i) it compiles and compares documented, DOI-verified quantitative evidence on nano-enhanced AC performance and multi-model ML sedimentation forecasting into a single comparative matrix; (ii) it formalizes the coupling between the two processes through three governing formulas — the Langmuir isotherm, a modified Stokes' law for nano-agglomerates, and a weighted ML ensemble equation; and (iii) it translates constructive procedures, tools and materials documented for United States full-scale deployments into a low-cost, modular configuration adapted to the topography, seasonality and resource constraints of Andean rivers, lakes and lagoons in Peru, illustrated with documented water-quality evidence from the Rimac and Ichu river basins.

2. Materials and Methods

This section describes the materials, computational tools and governing formulas used to build the proposed framework, together with the procedure used to compile and compare documented evidence from the United States and Peru. As this is a design-synthesis Method Article rather than a primary field or laboratory study, no new adsorption or sedimentation experiments were performed by the author; all quantitative values reported in Section 3 are drawn directly from the cited, DOI-verified sources.

2.1 Materials and tools considered

Adsorbent materials: granular activated carbon (GAC) derived from agricultural or forestry biomass, modified with graphene oxide (GO), nano zero-valent iron (nZVI), or metal/metal-oxide nanoparticles (e.g., Nb2O5, TiO2, Fe3O4), following the composite strategies documented by Chen et al. (2026), Bagheri et al. (2017) and Babaee et al. (2018). Computational tools: Python-based machine-learning libraries (scikit-learn, TensorFlow) for the multi-model ensemble, following the architecture documented by Le et al. (2024); open hydraulic/hydrological modelling environments for basin-scale flow characterization. Instrumentation: UV-Vis spectrophotometry and particle-size/turbidity sensors for in-line monitoring, consistent with the analytical approaches used in the cited adsorption and water-quality studies (Minga et al., 2023; Zárate-Cáceres et al., 2026).

2.2 Governing formulas

A. Adsorption isotherm (Langmuir model).

$$q_e = (q_{max} \cdot K_L \cdot C_e) / (1 + K_L \cdot C_e)$$

where qe is the amount of adsorbate at equilibrium (mg/g), qmax is the maximum monolayer adsorption capacity of the nano-enhanced AC (mg/g), KL is the Langmuir affinity constant (L/mg), and Ce is the

equilibrium concentration of the target contaminant in solution (mg/L). Reported qmax values for nitrogen-doped and composite ACs against pharmaceuticals such as acetaminophen reach on the order of 357 mg/g (Chen et al., 2026), illustrating the performance ceiling this formula is used to characterize.

B. Modified Stokes' law for nano-agglomerates.

$$v_s = [g \cdot (\rho_p - \rho_w) \cdot d_e^2 \cdot \chi] / (18 \cdot \mu)$$

where vs is the settling velocity of the sediment–nano-AC floc (m/s), g is gravitational acceleration (9.81 m/s²), ρp and ρw are the particle and water densities (kg/m³), de is the equivalent spherical diameter of the floc (m), μ is the dynamic viscosity of water (Pa·s), and χ is a sphericity/shape correction factor (χ ≤ 1) that accounts for the porosity and non-sphericity of fractal nano-agglomerates. Documented settling-time reductions of up to 86.4% upon aggregation of 23-nm nanoparticles into 2.5-μm clusters (Liyanage et al., 2016) illustrate why the correction factor χ cannot be omitted for nano-enhanced sediments, unlike in classical Stokes' law for rigid spheres.

C. Multi-model machine-learning ensemble.

$$\hat{v}_s = \Sigma_{i=1..n}\, w_i \cdot f_i(X)$$

$$w_i = (1/RMSE_i) / \Sigma_{k=1..n}\, (1/RMSE_k)$$

where fi(X) is the settling-velocity prediction of base model i (e.g., random forest, gradient boosting, categorical boosting, extra-tree regression) given input feature vector X (discharge, bed slope, flow width, grain-size percentiles, floc diameter), RMSEi is that model's root-mean-square error under cross-validation, and wi is its inverse-RMSE weight, following the weighted-averaging ensemble documented by Le et al. (2024), in which tree-based models achieved correlation scores above R = 0.936 while a Bayesian regression baseline reached only R = 0.838, underscoring the value of the ensemble over any single model.

2.3 Comparative procedure: United States practice versus proposed adaptation for Peru

In United States full-scale deployments, nano-enhanced AC is typically dosed in fixed or fluidized-bed contactors integrated with automated turbidity and UV-Vis monitoring, and settling-velocity forecasts feed centralized SCADA systems that schedule dredging or descolmatation cycles for reservoirs and engineered channels (Chen et al., 2026 review of composite AC deployments). This configuration assumes reliable grid power, continuous laboratory support and paved access for heavy dredging equipment. Andean rivers, lakes and lagoons in Peru present a different operating envelope: intermittent or absent grid power at high altitude, seasonal flow variability of the kind documented for the Rimac basin, steep and often unpaved access, and heavy-metal loads originating from legacy and active mining

activity that must be addressed jointly with organic micropollutants (Minga et al., 2023; Zárate-Cáceres et al., 2026).

The proposed adaptation therefore replaces fixed-bed contactors with modular, transportable AC cartridge banks fabricated from locally available biomass residues; replaces grid-powered SCADA with solar-powered programmable logic controllers (PLCs) driving low-power turbidity and UV-Vis sensors; and replaces centralized dredging scheduling with a field-deployable edge device running the same RF–gradient-boosting ensemble described in Section 2.2, retrained on locally collected discharge and sediment data before operational use. Figure 2 illustrates the resulting constructive layout, tools and material sequence.

2.4 Ethical statement and disclosure of language-model use

This manuscript is a literature-based engineering synthesis and design proposal; it does not involve human participants, animal subjects, identifiable personal data, or primary field sampling conducted by the author, and therefore formal research-ethics-committee approval is not applicable. All water-quality figures cited from the Rimac and Ichu basins are secondary data taken from the published, openly accessible sources listed in the References. In accordance with editorial policy on the use of large language models, an LLM was used exclusively for language editing, formatting and reference verification; the engineering framework, formula selection, comparative matrix design and interpretation were conceived and carried out by the author, who takes full responsibility for the content.

3. Results and Discussion

Because this article synthesizes rather than generates primary experimental data, the following results are documented values drawn from the cited, DOI-verified sources, organized into a comparative matrix (Table 1) that juxtaposes adsorption-material performance, multi-model sedimentation-forecasting accuracy, and Peruvian field water-quality evidence. No statistical inference is claimed beyond what is reported in the original sources; the matrix is offered as a synthesis tool to support the engineering framework proposed in Section 2, and any performance figures should be read as literature-documented benchmarks rather than as results of new experiments performed for this article.

3.1 Comparative matrix of documented quantitative evidence

Table 1
Comparative matrix of documented quantitative evidence on nano-enhanced activated-carbon adsorption performance, multi-model machine-learning sedimentation-forecasting accuracy, and Peruvian basin water-quality indicators, compiled from the cited DOI-verified sources.

Technology / system	Reported metric	Documented value	Source
AC + Nb2O5 nanoparticle composite (PET-derived, K2CO3-activated)	Removal of phenol, tetracycline and ciprofloxacin	≈ 60% at 10 wt% Nb loading; BET area 989 m²/g	Chen et al. (2026)
AC + TiO2/W composite (palm-kernel-shell derived)	Diclofenac removal under UV-B, with regeneration	74% removal; full capacity recovery after photocatalytic regeneration	Chen et al. (2026)
AZFC (activated ZIF-8 derivative)	Removal of 11 PFAS compounds (10 µg/L each)	85–99% removal; stable over ≥ 4 reuse cycles	Chen et al. (2026)
N-doped coconut-shell AC	Acetaminophen adsorption capacity / surface area	357.1 mg/g; 538 m²/g	Chen et al. (2026)
Multi-model ML ensemble (RF, GBM, CAT, ETR)	River bed-load / sediment-transport correlation	R > 0.936 (best models)	Le et al. (2024)
Bayesian Regression Model (single-model baseline)	Same sediment-transport prediction task	R = 0.838 (lowest of six models tested)	Le et al. (2024)
K-Nearest Neighbours model	Same sediment-transport prediction task	R ≈ 0.933	Le et al. (2024)
Nano-agglomeration of 23-nm nanoparticles	Brownian-motion settling-time reduction upon forming 2.5-µm aggregates	−86.44% settling time	Liyanage et al. (2016)
Rimac Basin – Parac subbasin, Peru (mining-influenced)	Heavy Metal Pollution Index (HPI) / HEI / Contamination degree (Cd)	Mean HPI 1378.5; HEI 134.5; Cd 126.5 (critical threshold = 100)	Minga et al. (2023)
Rimac Basin surface water, Peru	Arsenic and lead mean concentrations	As 0.02 mg/L; Pb 0.04 mg/L (exceeding limits at specific points)	Minga et al. (2023)
Ichu River, Peru	Dissolved-oxygen depletion linked to organic/mining pollution	6.3 → 4.5 mg/L across sampling sites	Zárate-Cáceres et al. (2026)

3.2 Framework architecture and constructive adaptation

Table 1 shows that composite AC materials reach removal efficiencies above 85% for structurally diverse contaminants (antibiotics, endocrine disruptors, PFAS) when nanomaterial functionalization is combined with adequate surface area, while tree-based multi-model ensembles consistently outperform single Bayesian baselines in sediment-transport prediction (R > 0.936 versus R = 0.838). These two documented performance patterns motivate the coupled architecture in Fig. 1, in which the adsorption

stage and the sedimentation-forecasting stage share instrumentation and feed a common multi-model ensemble that predicts the settling behaviour of the combined sediment–floc stream, rather than treating adsorption performance and settling prediction as independent design problems.

The Rimac and Ichu basin data in Table 1 indicate that Peruvian field conditions combine legacy mining-related heavy-metal loads (HPI up to an order of magnitude above the critical contamination threshold) with oxygen-depleting organic pollution, which is consistent with the dual adsorption–sedimentation problem the framework is designed to address, and justifies prioritizing nZVI- and GO-functionalized AC (documented for arsenic and dye removal by Babaee et al., 2018 and Bagheri et al., 2017) over simpler unmodified AC in the Peruvian configuration shown in Fig. 2.

3.3 Limitations

This article does not report new laboratory or field measurements; all adsorption and sedimentation-forecasting figures in Table 1 originate from the cited sources and were obtained under conditions (water matrices, contaminant mixtures, instrumentation, basin hydrology) that differ from those of Peruvian Andean systems. The multi-model ensemble described in Section 2.2 has been validated for river bed-load and suspended-sediment prediction in the source studies, but not yet retrained or field-validated on Peruvian discharge and sediment data. Direct comparability between the United States-documented composite-AC performance and its expected performance on Andean multi-pollutant, high-altitude waters should therefore be treated as a working hypothesis rather than an established result. Pilot-scale field validation in a Peruvian basin, with locally collected influent characterization and sediment gauging, is identified as the necessary next step before full-scale deployment.

4. Conclusions

This Method Article compiled documented, DOI-verified quantitative evidence on nano-enhanced activated-carbon adsorption and multi-model machine-learning sedimentation forecasting, and used it to construct an integrated engineering framework, formalized through the Langmuir isotherm, a modified Stokes' law for nano-agglomerates, and a weighted multi-model ensemble equation. The evidence compiled indicates that composite AC materials can remove 60–99% of structurally diverse emerging contaminants, that multi-model ML ensembles improve sediment-transport prediction accuracy over single-model baselines ($R > 0.936$ versus $R = 0.838$), and that Peruvian basins such as the Rimac and Ichu already exhibit heavy-metal pollution indices well above critical contamination thresholds alongside measurable oxygen depletion. Building on this evidence, constructive procedures, tools and materials documented for United States full-scale deployments were translated into a proposed low-cost, solar-powered, modular configuration adapted to the topography and resource constraints of Andean rivers, lakes and lagoons. The framework is a design and synthesis proposal; its central limitation is the absence of primary experimental validation on Peruvian systems, which is proposed as the immediate follow-up study.

References

1. Achite, M., Katipoğlu, O. M., Elshaboury, N., Tuğrul, T., & Pandey, K. (2025). Intercomparison of sediment transport curve and novel deep learning techniques in simulating sediment transport in the Wadi Mina Basin, Algeria. Environmental Earth Sciences, 84. https://doi.org/10.1007/s12665-024-12051-w
2. Babaee, Y., Mulligan, C. N., & Rahaman, M. S. (2018). Removal of arsenic (III) and arsenic (V) from aqueous solutions through adsorption by Fe/Cu nanoparticles. Journal of Chemical Technology & Biotechnology, 93(1), 63–71. https://doi.org/10.1002/jctb.5320
3. Bagheri, A. R., Ghaedi, M., Asfaram, A., Bazrafshan, A. A., & Jannesar, R. (2017). Comparative study on ultrasonic assisted adsorption of dyes onto Fe3O4 magnetite nanoparticles loaded on activated carbon. Ultrasonics Sonochemistry, 34, 294–304. https://doi.org/10.1016/j.ultsonch.2016.05.047
4. Bednárek, J., Matějová, L., Koutník, I., Vráblová, M., Cruz, G. J. F., Strašák, T., Šiler, P., & Hrbáč, J. (2024). Revelation of high-adsorption-performance activated carbon for removal of fluoroquinolone antibiotics from water. Biomass Conversion and Biorefinery, 14, 2585–2599. https://doi.org/10.1007/s13399-022-02577-z
5. Chen, H., Hu, Q., Huang, H., Chen, L., Zhang, C., Jin, Y., & Zhang, W. (2026). Adsorption and removal of emerging pollutants from water by activated carbon and its composites: Research hotspots, recent advances, and future prospects. Water, 18(3), 300. https://doi.org/10.3390/w18030300
6. Le, X.-H., Huynh, T. T., Song, M., & Lee, G. (2024). Quantifying predictive uncertainty and feature selection in river bed load estimation: A multi-model machine learning approach with particle swarm optimization. Water, 16(14), 1945. https://doi.org/10.3390/w16141945
7. Liyanage, C. D., Ratnayake, N. P., et al. (2016). An analysis of nanoparticle settling times in liquids. Journal of Nanomaterials, 2016, Article 7061838. https://doi.org/10.1155/2016/7061838
8. Minga, J. C., Elorza, F. J., Rodriguez, R., Iglesias, A., & Esenarro, D. (2023). Assessment of water resources pollution associated with mining activities in the Parac subbasin of the Rimac River. Water, 15(5), 965. https://doi.org/10.3390/w15050965
9. Sharafati, A., Haji Seyed Asadollah, S. B., Motta, D., & Yaseen, Z. M. (2020). Application of newly developed ensemble machine learning models for daily suspended sediment load prediction and related uncertainty analysis. Hydrological Sciences Journal, 65(12), 2022–2042. https://doi.org/10.1080/02626667.2020.1786571
10. Zárate-Cáceres, C. R., Iparraguirre-Meza, M., Pérez-Venegas, C. J., Picoy-Gonzales, J. A., Ordoñez-Ccora, G., Lacho-Gutiérrez, P., Riveros-Laurente, K. Y., Díaz-Aranda, D. L., Gutiérrez-Iparraguirre, G. G., Huarcaya-Taype, R., et al. (2026). Integrated water quality assessment and health risk analysis of heavy metal and microbial contamination in the Ichu River, Peru. F1000Research. https://doi.org/10.12688/f1000research.162022.4

Figures

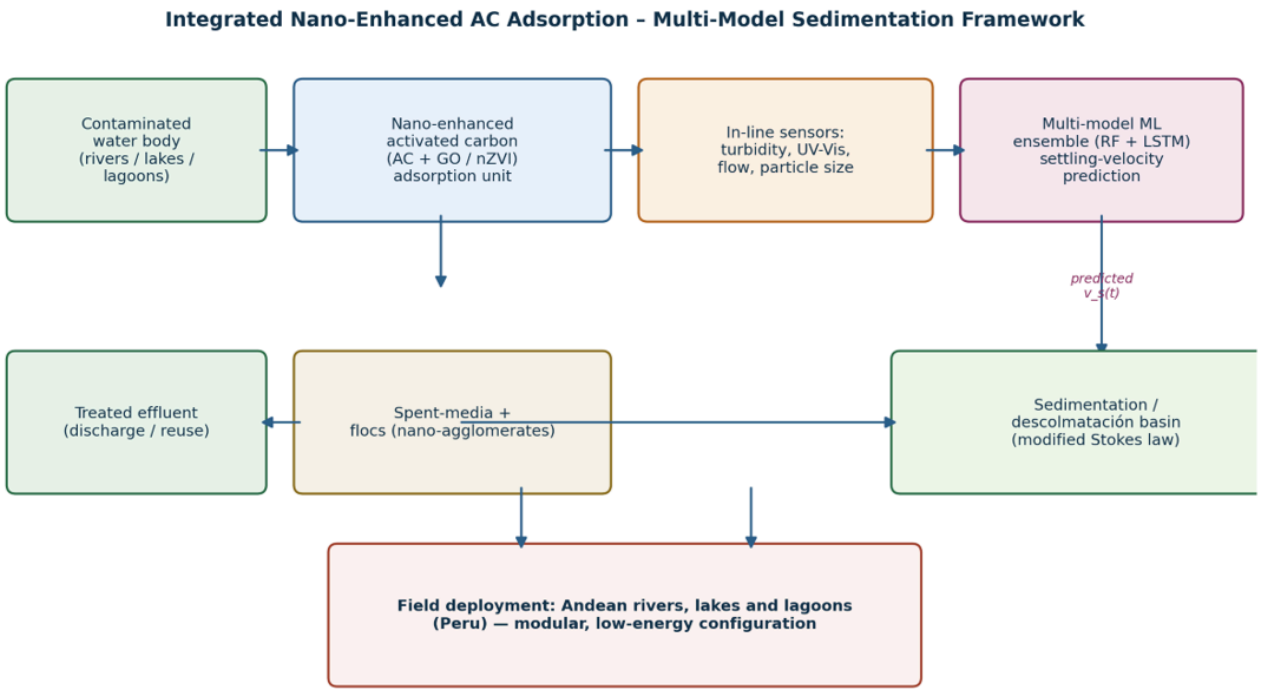


Figure 1. Schematic architecture of the nano-enhanced AC adsorption – multi-model sedimentation prediction framework, showing the adsorption stage, real-time sensing, machine-learning ensemble prediction, and sedimentation/descolmatation stage.

Figure 1

Schematic architecture of the nano-enhanced AC adsorption – multi-model sedimentation-prediction framework (Figure authored by Paul Ricardo Prudencio Galvez. All rights reserved.)

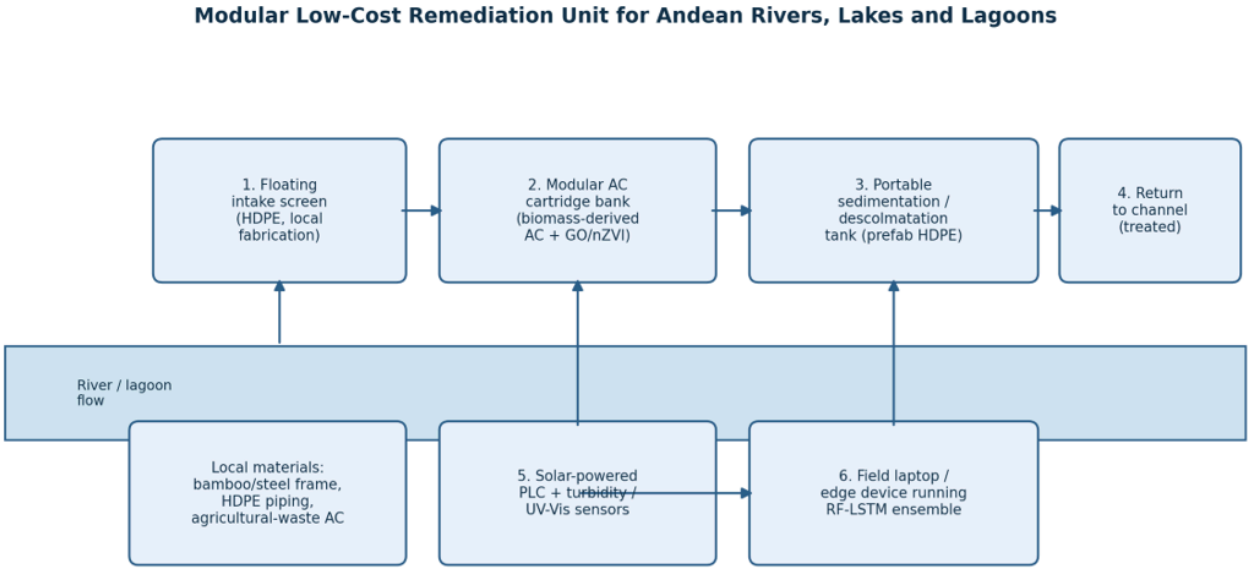


Figure 2. Constructive layout of the modular remediation unit proposed for deployment in Andean rivers, lakes and lagoons of Peru, indicating tools, materials and instrumentation sequence (adapted from the United States full-scale configuration).

Figure 2

Constructive layout, tools and materials proposed for deployment of the modular remediation unit in Andean rivers, lakes and lagoons of Peru (Figure authored by Paul Ricardo Prudencio Galvez. All rights reserved.)